Postnatal developmental changes in the sensitivity of L-type Ca^{2+} channel to inhibition by verapamil in a mouse heart model

Hironori Sagawa[1], Shinsuke Hoshino[2], Kengo Yoshioka[1], Wei-Guang Ding[1], Mariko Omatsu-Kanbe[1], Masao Nakagawa[2], Yoshihiro Maruo[2] and Hiroshi Matsuura[1]

BACKGROUND: In the clinical setting, verapamil is contraindicated in neonates and infants, because of the perceived risk of hypotension or bradyarrhythmia. However, it remains unclear whether there is an age-dependent difference in the sensitivity of cardiac L-type Ca^{2+} channel current ($I_{Ca,L}$) to inhibition by verapamil.

METHODS: Ventricular myocytes were enzymatically dissociated from the hearts of six different age groups (0, 7, 14, 21, 28 days, and 10–15 weeks) of mice, using a similar Langendorff-perfusion method. Whole-cell patch-clamp technique was applied to examine the sensitivity of $I_{Ca,L}$ to inhibition, by three classes of structurally different L-type Ca^{2+} channel antagonists.

RESULTS: Verapamil, nifedipine, and diltiazem concentration-dependently blocked the ventricular $I_{Ca,L}$ in all six age groups. However, although nifedipine and diltiazem blocked ventricular $I_{Ca,L}$ with a similar potency in all age groups, verapamil more potently blocked ventricular $I_{Ca,L}$ in day 0, day 7, day 14, and day 21 mice, than in day 28, and 10–15-week mice.

CONCLUSION: In a mouse heart model, ventricular $I_{Ca,L}$ before the weaning age (~21 days of age) exhibited a higher sensitivity to inhibition by verapamil than that after the weaning age, which may explain one possible mechanism associated with the development of verapamil-induced hypotension in human neonates and infants.

In the heart, the L-type Ca^{2+} channel current ($I_{Ca,L}$) plays a crucial role in the excitation–contraction coupling in ventricles and spontaneous automaticity in the sinoatrial and atrioventricular nodes (1,2). In the clinical setting, $I_{Ca,L}$ provides an important therapeutic target for the treatment of various cardiovascular disorders and diseases. Currently, three classes of structurally different L-type Ca^{2+} channel antagonists, namely dihydropyridines, benzothiazepines, and phenylalkylamines, are clinically used to treat tachyarrhythmia and hypertension (2,3). The phenylalkylamine verapamil is effective in terminating paroxysmal supraventricular tachycardia and some forms of ventricular tachycardia in adults (4,5). However, the intravenous administration of verapamil has been regarded as contraindicated in neonates and infants (4,6), because of a substantial risk of severe hypotension or bradycardia (7). In contrast, it is generally accepted that the dihydropyridines (nifedipine and isradipine) and benzothiazepine diltiazem can be safely used in neonates and infants in the clinical setting, without causing significant hypotension (8–10).

Previous studies have shown that the expression and function of Ca^{2+} handling proteins, involved in excitation–contraction coupling in the heart, undergo significant changes during postnatal development (11,12). For example, current density of $I_{Ca,L}$ exhibits a postnatal developmental increase in many mammalian species, including mouse and rabbit (13–15). In contrast, the expression of Na^+/Ca^{2+} exchanger is highest in neonatal stages, and then gradually decreases during postnatal development in the hearts of rabbits and rats (16,17). It is also known that, because the sarcoplasmic reticulum and transverse tubules are less developed in the neonatal stage than in adult stage (11,18), the transsarcolemmal Ca^{2+} influx through $I_{Ca,L}$ and/or the reverse mode Na^+/Ca^{2+} exchanger plays a predominant role in providing the Ca^{2+} required for cardiomyocyte contraction (19,20). Indeed, it has been demonstrated in rabbit that myocardial contractile force in immature hearts is more sensitive to the L-type Ca^{2+} channel antagonists (verapamil, nifedipine, and diltiazem) than that in the adult hearts (21,22).

However, it remains unclear how phenylalkylamine verapamil exerts its more potent negative inotropic action in neonates and infants than dihydropyridines and benzothiazepines. The present study was undertaken to examine the possible postnatal developmental changes in the sensitivity of $I_{Ca,L}$ to the inhibition by verapamil. Our results revealed that verapamil more potently inhibits $I_{Ca,L}$ in ventricular myocytes of mice before the weaning age (~21 days after birth) than in mice after the weaning age.

METHODS

Mice at Various Postnatal Ages

Mice on the day of birth were denoted as postnatal day 0 in age. We used six different age groups (day 0, day 7, day 14, day 21, day 28, and 10–15 weeks) of mice (C57BL/6J; Charles River, Yokohama,

[1]Department of Physiology, Shiga University of Medical Science, Otsu, Shiga, Japan; [2]Department of Pediatrics, Shiga University of Medical Science, Otsu, Shiga, Japan. Correspondence: Hiroshi Matsuura (matuurah@belle.shiga-med.ac.jp)

Received 29 August 2017; accepted 29 January 2018; advance online publication 18 April 2018. doi:10.1038/pr.2018.46

Japan) for the experiments investigating the blocking actions of verapamil, nifedipine, and diltiazem on $I_{Ca,L}$. Because mice are usually weaned ~21 days after birth (23), we may reasonably assume that mice younger than 21 days after birth correspond to neonatal and infant stages in humans. In contrast, mice at 28 days and 10–15 weeks after birth can be regarded as representing child and adult stages in humans, respectively (24). All protocols conformed to the Guide for the Care and Use of Laboratory Animals published by the US National Institutes of Health (NIH Publication No. 85-23, revised 1996), and were approved by the institution's Animal Care and Use Committee of Shiga University of Medical Science (approval number, 2014-8-2).

Isolation of Ventricular Myocytes

Ventricular myocytes were enzymatically dissociated from the hearts of mice in all age groups (0, 7, 14, 21, 28 days, and 10–15 weeks) using a similar Langendorff-perfusion method (15,25,26). Mice were killed by an intraperitoneal injection of sodium pentobarbital overdose (300 mg/kg) with heparin (8,000 U/kg). In all age groups, the heart was rapidly removed and perfused at 37 °C for 3 min in a Langendorff mode with cell isolation buffer (CIB), supplemented with 0.4 mM EGTA. The CIB contained (in mM) 130 NaCl, 5.4 KCl, 0.5 $MgCl_2$, 0.33 NaH_2PO_4, 22 glucose, 25 HEPES (pH adjusted to 7.4 with NaOH), and 50 U/ml bovine insulin. The hearts of day 0 and day 7 mice were then perfused for 3–5 min with CIB supplemented with 1 mg/ml collagenase (type 2; Worthington Biochemical Corporation, Lakewood, NJ), 0.03 mg/ml trypsin (Sigma, St. Louis, MO), 0.03 mg/ml protease (Sigma), and 0.15 mM $CaCl_2$. The heart was then removed from the Langendorff apparatus, and the ventricles were gently agitated to disperse the myocytes in CIB, supplemented with 1.2 mM $CaCl_2$ and 2 mg/ml bovine serum albumin (BSA, Sigma). The hearts of day 14, day 21, day 28, and 10–15-week mice were Langendorff-perfused for 6–8 min with CIB supplemented with 1 mg/ml collagenase, 0.06 mg/ml trypsin, 0.06 mg/ml protease, and 0.3 mM $CaCl_2$. The hearts were removed from the Langendorff apparatus, chopped into small pieces, and further incubated at 37 °C for 10 min in CIB supplemented with 1 mg/ml collagenase, 0.03 mg/ml trypsin, 0.03 mg/ml protease, 0.7 mM $CaCl_2$, and 2 mg/ml BSA. The supernatant was centrifuged (14*g* for 3 min), and the myocyte pellet was resuspended in CIB supplemented with 1.2 mM $CaCl_2$ and 2 mg/ml BSA. The myocytes were further incubated for 10 min, centrifuged (14*g* for 3 min), and resuspended in normal Tyrode solution supplemented with 2 mg/ml BSA. The normal Tyrode solution contained (in mM) 140 NaCl, 5.4 KCl, 1.8 $CaCl_2$, 0.5 $MgCl_2$, 0.33 NaH_2PO_4, 5.5 glucose, and 5.0 HEPES (pH adjusted to 7.4 with NaOH). It should be noted that chunk method has been commonly used to isolate ventricular myocytes having spherical shape from neonatal mice, possibly because of the technical difficulty in introducing the Langendorff-perfusion method. The present investigation adopted the Langendorff-perfusion method, which enables the harvesting of spindle- or rod-shaped healthy ventricular myocytes from neonatal mice (15).

Whole-cell patch-clamp experiments

The whole-cell patch-clamp technique (27) was used to record $I_{Ca,L}$ in mouse ventricular myocytes of all age groups, with an EPC-8 patch-clamp amplifier (HEKA, Lambrecht, Germany). The patch electrodes, fabricated from glass capillaries using a horizontal microelectrode puller (P-97; Sutter Instrument, Novato, CA), had a resistance of 2.0–4.0 MΩ, when filled with a Cs^+-rich pipette solution that contained (in mM) 90 cesium aspartate, 30 CsCl, 20 tetraethylammonium chloride, 2 $MgCl_2$, 5 ATP (magnesium salt; Sigma), 0.1 GTP (dilithium salt; Roche Diagnostics, GmbH, Mannheim, Germany), 5 phosphocreatine (disodium salt; Sigma), 5 EGTA, and 5 HEPES (pH adjusted to 7.2 with CsOH). Ventricular myocytes were transferred to a recording chamber (0.5 ml in volume) mounted on the stage of an inverted microscope, and continuously superfused at 36–37 °C with normal Tyrode solution. After the establishment of whole-cell patch-clamp mode, ventricular myocytes were superfused with a Cs^+-Tyrode solution containing (in mM) 140 NaCl, 5.4 CsCl, 1.8 $CaCl_2$, 0.5 $MgCl_2$, 5.5 glucose, and 5 HEPES (pH adjusted to 7.4 with NaOH). $I_{Ca,L}$ was activated by depolarizing voltage-clamp steps applied from a holding potential of −40 mV to test potentials of −30 mV through +40 mV in 10 mV steps, before and during exposure to verapamil (hydrochloride, 10^{-8} to 10^{-6} M; Sigma), nifedipine (10^{-9} to 10^{-7} M; Sigma), or diltiazem (hydrochloride, 10^{-8} to 10^{-6} M; Sigma). In experiments examining the blocking effects of these L-type Ca^{2+} channel antagonists, only one concentration of the drug was tested in each ventricular myocyte. The percentage reduction in the amplitude of $I_{Ca,L}$ was measured at 0 mV by the presence of each test concentration of the drug, and was fitted with a Hill equation: $R = 100/(1+(IC_{50}/[\text{drug}])^{nH})$, where R is the percent reduction of $I_{Ca,L}$, IC_{50} is the concentration of drug causing a half-maximal inhibition, and nH is a Hill coefficient. The conductance of $I_{Ca,L}$ ($g_{Ca,L}$) was calculated by dividing the current amplitude at each test potential by the driving force for Ca^{2+} influx through $I_{Ca,L}$ and was then normalized with the maximum value at +10 or +20 mV ($g_{Ca,L}$,max) (15,28). The normalized conductance ($g_{Ca,L}$) was fitted with a Boltzmann equation: $g_{Ca,L} = 1/(1+\exp((V_{1/2}-V_t)/k))$, where $V_{1/2}$ is the voltage at half-maximal activation, V_t is test potential, and k is the slope factor. Frequency-dependent block of $I_{Ca,L}$ by verapamil, nifedipine, or diltiazem was evaluated in ventricular myocytes of day 7 and 10–15-week mice by repetitively (0.2 or 2 Hz) applying depolarizing steps to 0 mV from a holding potential of −40 mV in the presence of verapamil, nifedipine, or diltiazem. The concentration of verapamil, nifedipine, or diltiazem was set to near the IC_{50} values for the inhibition by each antagonists; verapamil (50 nM for day 7 and 150 nM for 10–15-week ventricular myocytes), nifedipine (10 nM for both day 7 and 10–15-week ventricular myocytes), and diltiazem (150 nM for both day 7 and 10–15-week ventricular myocytes). Cell membrane capacitance (C_m) was measured from the capacitive transients in response to voltage-clamp steps (±5 mV) applied from a holding potential of −40 mV, using the follow equation; $C_m = \tau_C\, I_0/\Delta V_m\, (1 - I_\infty/I_0)$ (15,29), where τ_C is the time constant of the capacitive transient, I_0 is the initial peak current amplitude, I_∞ is the steady-state current value, ΔV_m is the amplitude of voltage step (5 mV).

Western Blotting and Immunocytochemistry

A full description of western blotting and immunocytochemistry, including primary antibodies used for these experiments, is available in Methods in online **Supplementary Information**.

Statistical Analysis

Data are presented as mean ± SD. Statistical significance was evaluated using either Student's unpaired *t*-test or an analysis of variance, followed by a *post hoc* Dunnett or Tukey test, as appropriate. A value of $P < 0.05$ was considered to be statistically significant.

RESULTS

Electrophysiological Properties of $I_{Ca,L}$ in Ventricular Myocytes Isolated from Different Age Groups of Mouse Heart

We first examined the cell membrane capacitance (C_m) of ventricular myocytes isolated from the hearts of six different age groups (0, 7, 14, 21, 28 days, and 10–15 weeks) of mice. As shown in **Figure 1**, C_m, which is proportional to the cell surface area, increased from 20.7 ± 8.3 pF ($n = 44$) in day 0 ventricular myocytes to 142.6 ± 10.7 pF ($n = 75$) in 10–15-week ventricular myocytes. These values of C_m are qualitatively similar to the previous observations in mouse ventricular myocytes and indicate that the ventricular cell size gradually increases with postnatal growth of the heart (15,30).

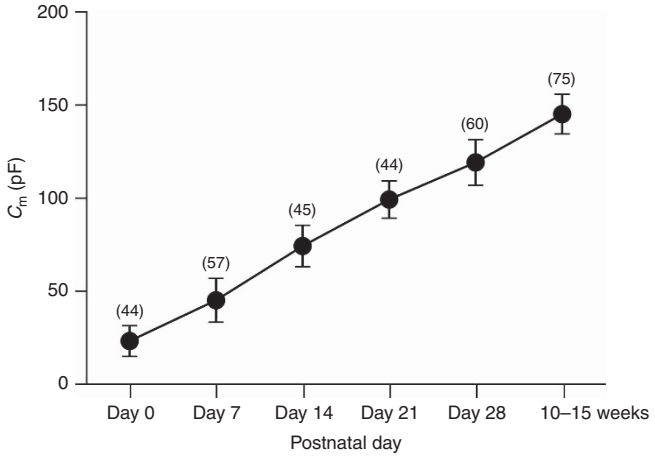

Figure 1. Postnatal developmental increases in ventricular cell size. Cell membrane capacitance (C_m) of ventricular myocytes obtained from six different age groups from day 0 to 10–15 weeks. Data represent mean ± SD (number of cells).

We then investigated the conductance properties of $I_{Ca,L}$ in mouse ventricular myocytes of all age groups. As described in **Figure 2a,b**, $I_{Ca,L}$ exhibited its maximum amplitude at a test potential of −10 or 0 mV in both postnatal day 0 and 10–15-week ventricular myocytes. However, the maximum amplitudes of $I_{Ca,L}$, measured at a test potential of −10 or 0 mV, gradually increased during postnatal development from 4.8 ± 0.9 pA/pF ($n = 8$) in day 0 to 11.0 ± 2.2 pA/pF ($n = 8$) in 10–15-week ventricular myocytes (**Figure 2c**), consistent with the previous study (15). The conductance of $I_{Ca,L}$ at each test potential was then calculated by dividing the peak amplitude of $I_{Ca,L}$ by the driving force for Ca^{2+} influx through $I_{Ca,L}$. The smooth curves through the data points represent the least-squares fit of the Boltzmann equation (**Figure 2d**), yielding $V_{1/2}$ and k. There were no significant differences in the values of $V_{1/2}$ (**Figure 2e**) or k (**Figure 2f**) among all age groups, suggesting that the voltage-dependence of $I_{Ca,L}$ activation does not differ during the postnatal development of mice from day 0 through 10–15 weeks. Previous studies have also shown that there are no significant developmental changes in the voltage-dependence of $I_{Ca,L}$ activation in ventricular myocytes from neonatal to adult stages in mouse and rabbit (13–15).

Postnatal Developmental Changes in the Sensitivity of $I_{Ca,L}$ to the Inhibition by Verapamil

We next investigated the pharmacological sensitivity of $I_{Ca,L}$ in ventricular myocytes at various developmental stages to three structurally different L-type Ca^{2+} channel antagonists; namely phenylalkylamine verapamil, dihydropyridine nifedipine, and benzodiazepine diltiazem. **Figure 3a** shows the superimposed current traces of $I_{Ca,L}$ recorded at test potentials of −30 through +40 mV in days 0, 7, 14, 21, 28, and 10–15-week ventricular myocytes before and during exposure to 100 nM verapamil. Under control conditions, the amplitude of $I_{Ca,L}$ was maximum at test potentials of −10 or 0 mV in all of these ventricular myocytes (**Figure 3b**). Verapamil (100 nM) was found to reduce $I_{Ca,L}$ in all developmental stages, which appeared, however, more potent in younger stages than in older ones.

To quantitatively analyze the blocking effect of verapamil on $I_{Ca,L}$, we measured the percentage inhibition of $I_{Ca,L}$ by various concentrations (10^{-8} to 10^{-6} M) of verapamil at a test potential of 0 mV in ventricular myocytes of all developmental stages. The potency of verapamil in blocking $I_{Ca,L}$ was examined by constructing the concentration–response relationships for the percent inhibition of $I_{Ca,L}$ by verapamil in days 0, 7, 14, 21, 28, and 10–15-week ventricular myocytes (**Figure 4a**). As summarized in **Figure 4d**, IC_{50} value for the inhibition of $I_{Ca,L}$ in days 0, 7, 14, 21 ventricular myocytes was smaller than that in day 28 and 10–15-week ventricular myocytes, showing that verapamil inhibits $I_{Ca,L}$ more potently in ventricular myocytes at younger stages than at older stages. However, there were no significant changes in IC_{50} value for the blocking action of nifedipine on $I_{Ca,L}$ among ventricular myocytes at any developmental stages (**Figure 4b,e**). Similarly, IC_{50} value for diltiazem did not differ among ventricular myocytes at any developmental stage (**Figure 4c,f**).

Frequency-Dependent Blocking Property of Verapamil on $I_{Ca,L}$

Verapamil, nifedipine, and diltiazem have been shown to exhibit differential frequency-dependent block of $I_{Ca,L}$ in heart cells (31–33). We then investigated the frequency-dependent blocking property of verapamil, nifedipine, or diltiazem on $I_{Ca,L}$ in ventricular myocytes of day 7 and 10–15-week mice. For this purpose, verapamil was applied to the ventricular myocytes of day 7 and 10–15-week mice at concentrations near to their respective IC_{50} values to block $I_{Ca,L}$ (50 nM and 150 nM for day 7 and 10–15-week ventricular myocytes, respectively). Ventricular myocytes were repetitively depolarized from a holding potential of −40 mV to a test potential of 0 mV in the presence of verapamil at a frequency of 0.2 and 2 Hz. As demonstrated in **Figure 5a**, the amplitude of $I_{Ca,L}$ at the 15th step applied at 0.2 Hz was moderately reduced, compared with that at the 1st step in both day 7 and 10–15-week ventricular myocytes. In contrast, the amplitude of $I_{Ca,L}$ at the 15th step applied at 2 Hz was markedly reduced, compared with the 1st step in both day 7 and 10–15-week ventricular myocytes (**Figure 5b**).

Figure 5c summarizes the changes in the peak amplitude of $I_{Ca,L}$ during the trains of 15 depolarizing steps applied at 0.2 and 2 Hz in the presence of verapamil in day 7 (left panel) and 10–15-week (right panel) ventricular myocytes. Using the same protocol, we measured the changes in the peak amplitude of $I_{Ca,L}$ in the presence of nifedipine (10 nM, **Figure 5d**) or diltiazem (150 nM, **Figure 5e**) in day 7 (left panel) and 10–15-week (right panel) ventricular myocytes. To assess the frequency-dependent block by verapamil, nifedipine, or diltiazem, the peak amplitude of $I_{Ca,L}$ at the 15th step (I_{15}) was normalized to that at the 1st step (I_1), and this ratio in current amplitudes (I_{15}/I_1) was compared at frequencies of 0.2 and 2 Hz. In both day 7 and 10–15-week ventricular

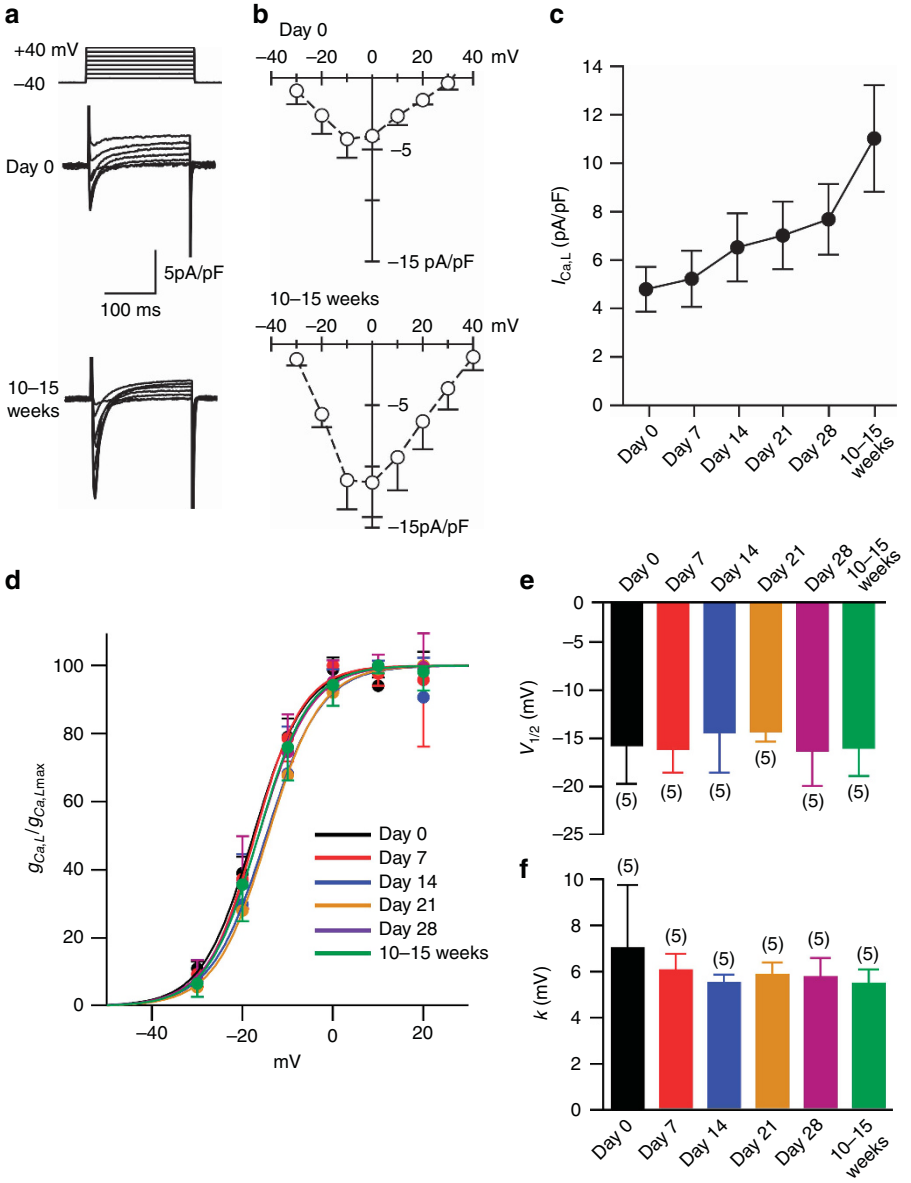

Figure 2. Conductance property of $I_{Ca,L}$ in mouse ventricular myocytes. (**a**) Superimposed current traces of $I_{Ca,L}$ recorded during depolarizing steps applied from a holding potential of − 40 mV to test potentials of –30 to +40 mV, from day 0 (upper panel) and 10–15-week (lower panel) ventricular myocytes. (**b**) Mean current–voltage relationships for peak $I_{Ca,L}$, obtained from day 0 (upper panel, $n = 5$) and 10–15-week (lower panel, $n = 5$) ventricular myocytes. (**c**) Postnatal increase in the maximal amplitude of $I_{Ca,L}$ from day 0 to 10–15-week ventricular myocytes. (**d**) Mean normalized conductance–voltage relationships for $I_{Ca,L}$ in ventricular myocytes of all postnatal stages. Data points were fitted with the Boltzmann equation. $V_{1/2}$ (**e**) and k (**f**) obtained from the Boltzmann fit shown in **d**. The number of cells is indicated in parentheses. Note that there are no significant differences in $V_{1/2}$ and k among all age groups.

myocytes, the ratio of I_{15}/I_1 obtained at 2 Hz was significantly smaller than that at 0.2 Hz in verapamil and diltiazem (Figure 5f), suggesting that a frequency-dependent block of $I_{Ca,L}$ was observed for these two antagonists in both day 7 and 10–15-week ventricular myocytes. However, there was no significant change in I_{15}/I_1 obtained at 0.2 or 2 Hz in nifedipine (Figure 5f), suggesting that a frequency-dependent block of $I_{Ca,L}$ was scarcely observed for this antagonist in both day 7 and 10–15-week ventricular myocytes.

Expression and Cellular Localization of $Ca_V1.2$ and $Ca_V1.3$ Channel Proteins in Day 7 and 10–15-Week Ventricular Myocytes

It has been demonstrated in the mouse heart that although $Ca_V1.2$ channel primarily contributes to $I_{Ca,L}$ in adult ventricular myocytes, $Ca_V1.3$ channel is mainly responsible for $I_{Ca,L}$ in the early embryonic ventricular myocytes (34). It is, however, still unknown whether $Ca_V1.3$ channel is expressed in mouse ventricular myocytes at early postnatal stages. We therefore examined the expression of $Ca_V1.2$ and

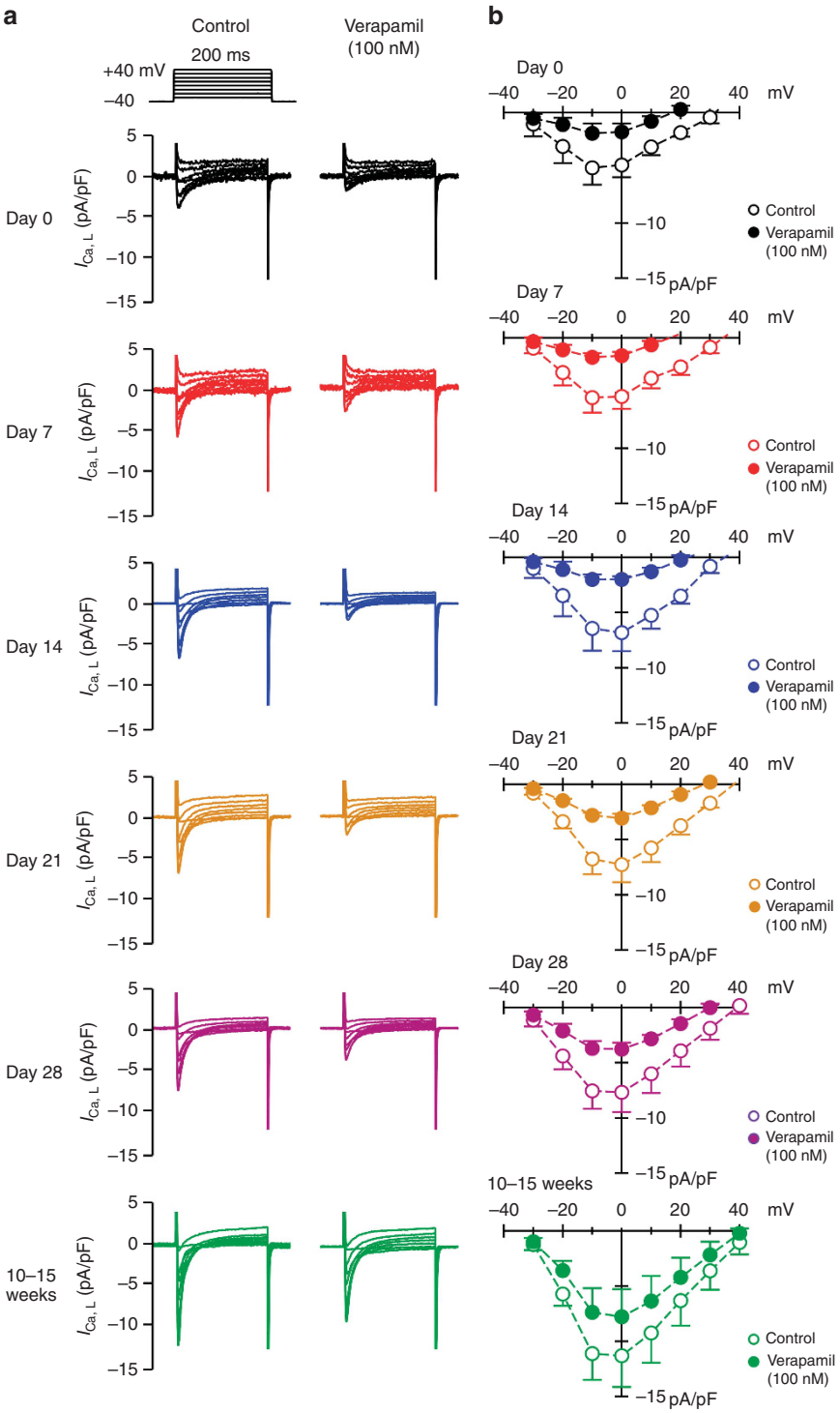

Figure 3. $I_{Ca,L}$ recorded from the ventricular myocytes of various developmental stages in the absence and presence of 100 nM verapamil. (**a**) Superimposed current traces of $I_{Ca,L}$ recorded during 200-ms depolarizing steps to test potentials of –30 to +40 mV, before and 2–3 min after exposure to 100 nM verapamil. (**b**) Current–voltage relationships for $I_{Ca,L}$ measured before (empty symbols) and after (filled symbols) the exposure to 100 nM verapamil.

$Ca_V1.3$ channel proteins in day 7 and 10–15-week ventricular myocytes, using Western blotting and immunocytochemistry. $Ca_V1.2$ channel protein was detected by Western blotting in both day 7 and 10–15-week ventricular myocytes (Figure 6a). On the other hand, $Ca_V1.3$ channel protein was detected in day 7 ventricular myocytes, but was not clearly observed in 10–15-week ventricular myocytes (Figure 6b). Immunocytochemistry confirmed that $Ca_V1.2$ channel was expressed in both day 7 and 10–15-week ventricular myocytes (Figure 6c). A merged image of the immunofluorescent

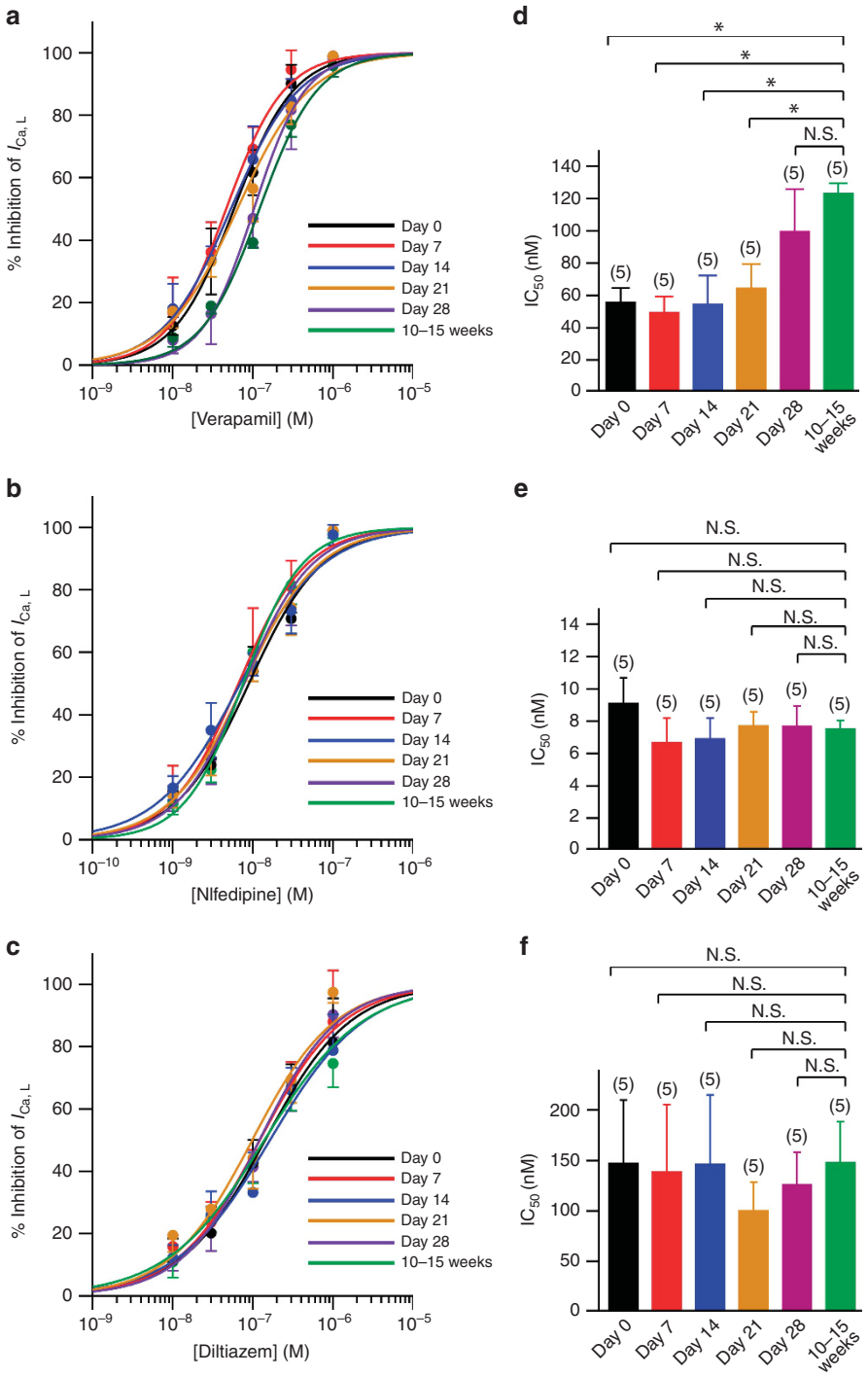

Figure 4. Blocking potency of verapamil, nifedipine, and diltiazem on $I_{Ca,L}$ in ventricular myocytes of all developmental stages. (**a**–**c**) The concentration–response relationships for the inhibition of $I_{Ca,L}$ by verapamil (**a**), nifedipine (**b**), and diltiazem (**c**). The percent inhibition of $I_{Ca,L}$ by verapamil, nifedipine, and diltiazem, measured at 0 mV, was plotted against their concentrations. (**d**–**f**) IC_{50} for the block of $I_{Ca,L}$ by verapamil (**d**), nifedipine (**e**), and diltiazem (**f**). Note that the blocking potency of verapamil on $I_{Ca,L}$ was stronger in day 0, day 7, day 14, and day 21 ventricular myocytes than in day 28 and 10–15-week ventricular myocytes. *$P < 0.05$ compared with 10–15-week ventricular myocytes. N.S., not significant.

signals of $Ca_V1.2$ channel and α-actinin in both day 7 and 10–15-week ventricular myocytes indicated that this channel was orderly expressed along with the sarcomeres. In contrast, the immunofluorescent signals of $Ca_V1.3$ channel were not detected in 10–15-week ventricular myocytes. In day 7 ventricular myocytes, the immunofluorescent signals of $Ca_V1.3$ channel were only detected in the perinuclear area (Figure 6d). A similar perinuclear localization of $Ca_V1.3$ channel has been reported in the neonatal rat ventricular myocytes (35).

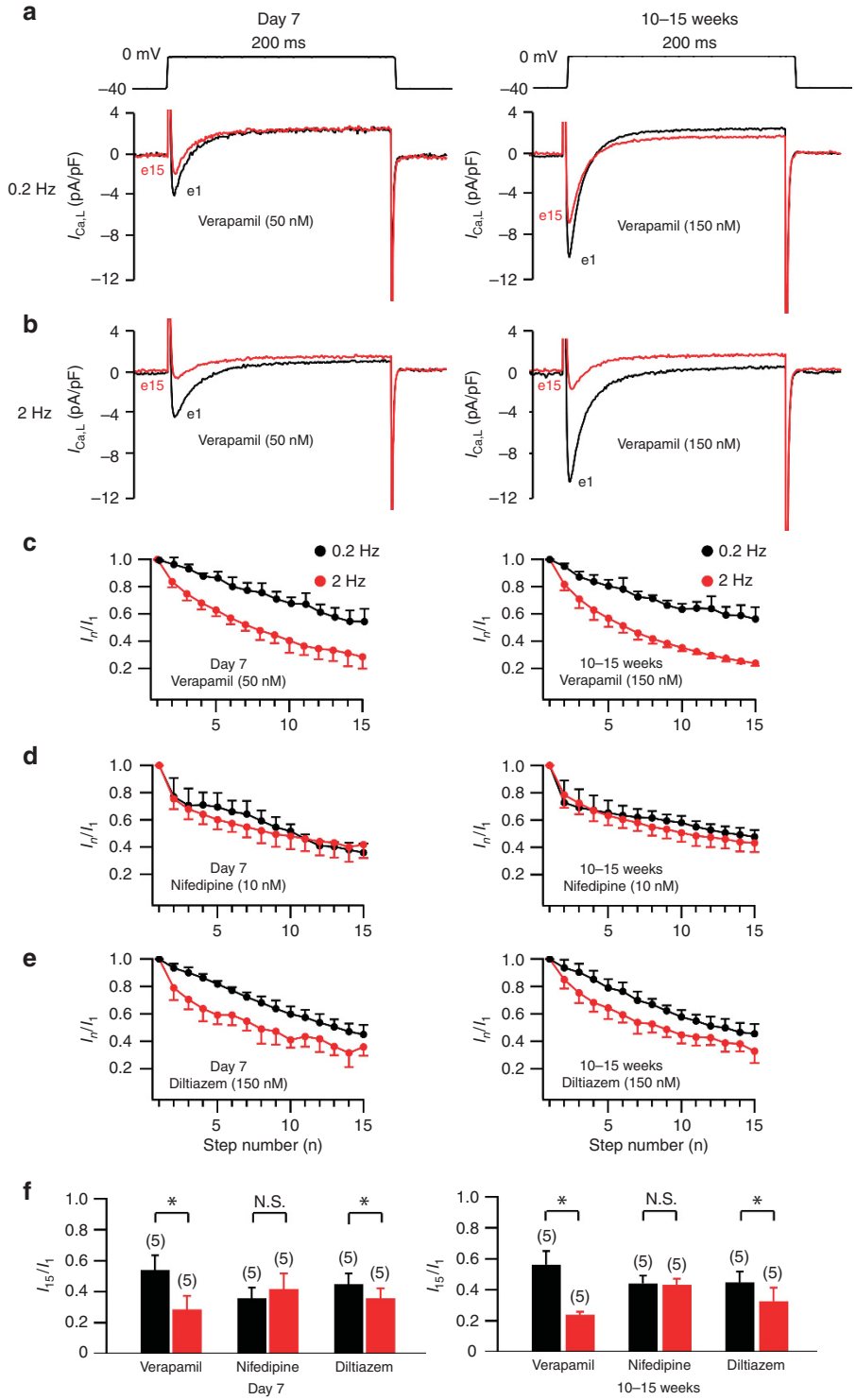

Figure 5. Frequency-dependent block of $I_{Ca,L}$ by verapamil, nifedipine, or diltiazem in ventricular myocytes of day 7 and 10–15-week mice. Depolarizing voltage-clamp steps were applied to a test potential of 0 mV from a holding potential of −40 mV at a frequency of 0.2 or 2 Hz in the presence of verapamil, nifedipine, or diltiazem. The concentration of verapamil, nifedipine, or diltiazem was set to near the IC_{50} value for inhibition by verapamil (50 nM for day 7 or 150 nM for 10–15-week ventricular myocytes), nifedipine (10 nM for both day 7 and 10–15-week ventricular myocytes), or diltiazem (150 nM for both day 7 and 10–15-week ventricular myocytes). (**a**, **b**) Superimposed current traces of $I_{Ca,L}$ at the 1st and 15th depolarizing steps applied at a frequency of 0.2 Hz (**a**) or 2 Hz (**b**) in the presence of verapamil in day 7 (left panel) and 10–15-week (right panel) ventricular myocytes. (**c**–**e**) The peak amplitude of $I_{Ca,L}$ at each depolarizing step applied at 0.2 and 2 Hz was normalized with reference to the value at the first step (I_n/I_1) and plotted against the step number in the presence of verapamil (**c**), nifedipine (**d**), or diltiazem (**e**) in day 7 (left panel) and 10–15-week (right panel) ventricular myocytes. (**f**) The relative amplitude of $I_{Ca,L}$ at the 15th step to that at the 1st step at a frequency of 0.2 and 2 Hz in the presence of verapamil, nifedipine, or diltiazem in day 7 (left panel) and 10–15-week (right panel) ventricular myocytes. *$P < 0.05$. N.S., not significant.

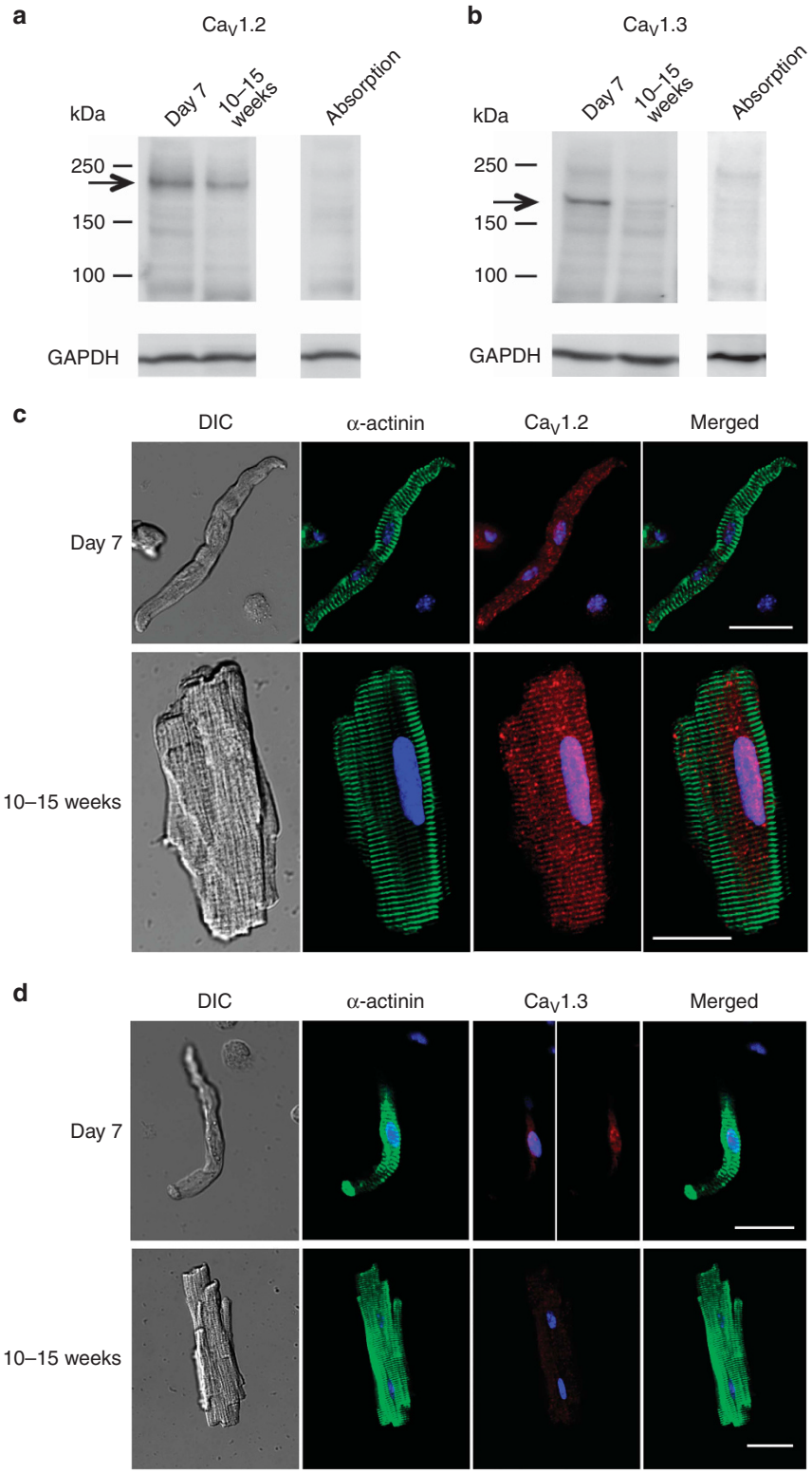

Figure 6. Expression and cellular localization of $Ca_V1.2$ and $Ca_V1.3$ channel proteins in day 7 and 10–15-week mouse ventricles. (**a, b**) Western blotting of $Ca_V1.2$ (**a**) and $Ca_V1.3$ (**b**) channel expression in day 7 and 10–15-week ventricular tissues. $Ca_V1.2$ and $Ca_V1.3$ channel antibodies preincubated with control peptide antigen in day 7 mouse ventricular tissue (absorption test). GAPDH was used as an internal control. (**c**, **d**) Confocal laser scanning microscopy of double immunostaining for α-actinin and $Ca_V1.2$ (**c**), or $Ca_V1.3$ (**d**) channel, DAPI staining for nuclei and differential interference contrast (DIC) images of day 7 and 10–15-week ventricular myocytes. Bar = 25 μm.

DISCUSSION

Previous studies have shown that excitation–contraction coupling in the heart undergoes significant postnatal developmental changes in experimental animals (11,12). Because of the poor development of sarcoplasmic reticulum and transverse tubules, the transsarcolemmal Ca^{2+} influx appears to be a more important source of Ca^{2+} to trigger the contraction of cardiac myocytes than Ca^{2+} release from the sarcoplasmic reticulum (19,20). Indeed, the blockade of $I_{Ca,L}$ by verapamil and diltiazem has been reported to produce more potent negative inotropic action in the neonatal rabbit hearts than in the adult rabbit hearts (22). However, the precise mechanism mediating the more marked inhibitory effect of verapamil on cardiac contractile function in the immature heart than that of dihydropyridine and benzothiazepine classes of L-type Ca^{2+} channel antagonists has yet to be fully elucidated.

The present experiments using a mouse heart model revealed that, although the sensitivity of $I_{Ca,L}$ to inhibition by nifedipine or diltiazem are similar at all developmental stages, the sensitivity of $I_{Ca,L}$ to verapamil is higher in mice of ≤ 21 days of age than in those of ≥ 28 days of age (**Figure 4**). Thus, this study showed for the first time that postnatal developmental changes in the sensitivity of $I_{Ca,L}$ are present in verapamil, but not in nifedipine or diltiazem. In the clinical setting, the maximum concentration of free verapamil in the serum has been reported to be approximately 80 nM (36), where a substantial difference in the degree of $I_{Ca,L}$ inhibition was observed between the neonatal and adult ventricular myocytes (~60% and 40% inhibition in day 0 and 10–15-week mice, respectively; **Figure 4a**). This difference might be involved in the differential sensitivity of ventricular contractile function to verapamil between neonates and adults.

Four pore-forming α subunits of $I_{Ca,L}$ channel have been identified, namely, $Ca_V1.1$ (α_{1S}), $Ca_V1.2$ (α_{1C}), $Ca_V1.3$ (α_{1D}), and $Ca_V1.4$ (α_{1F}) (1,2). Among these, $Ca_V1.2$ and $Ca_V1.3$ channels underlie $I_{Ca,L}$ in mammalian ventricles (34). It has been shown in mouse ventricular myocytes that $Ca_V1.3$ channel is functionally expressed at the early embryonic stages; however, it is gradually downregulated during the second-half of the embryonic stage, leading to a negligibly low expression level at 18 days post coitum (34). In contrast, the expression of $Ca_V1.2$ channel is gradually increased throughout the embryonic stages (34,37), and hence $Ca_V1.2$ channel becomes the predominant isoform at 18 days post coitum, which continues thereafter (34). In the present study, Western blotting and immunocytochemistry revealed that $Ca_V1.2$ channel is expressed in sarcomeres in both day 7 and 10–15-week ventricular myocytes (**Figure 6a,c**), supporting the view that the $Ca_V1.2$ channel is functionally expressed in the ventricular myocytes of both ages.

On the other hand, although the expression of $Ca_V1.3$ channel in day 7 ventricular myocytes was detected by Western blotting (**Figure 6b**), the $Ca_V1.3$ channel was found to be mainly localized in the perinuclear region, and was scarcely detected in the plasma membrane by immunocytochemistry (**Figure 6d**). It therefore seems likely that the functional expression of $Ca_V1.3$ channel is minimal in day 7 mouse ventricular myocytes. Consistent with a previous study using mouse ventricular myocytes (34), the expression of $Ca_V1.3$ channel was not detected in 10–15-week ventricular myocytes by either Western blotting or immunocytochemistry (**Figure 6b,d**). Taken together, it seems reasonable and plausible to assume that $I_{Ca,L}$ recorded from mouse ventricular myocytes in various postnatal stages in the present study was primarily based on $Ca_V1.2$ channel rather than $Ca_V1.3$ channel.

Previous studies have shown that $Ca_V1.3$ channel activates at a more negative membrane potential than $Ca_V1.2$ channel, and exhibits less sensitivity to dihydropyridines than $Ca_V1.2$ channel (38,39). The present study confirms that there were no significant differences in both the voltage dependence of $I_{Ca,L}$ activation (**Figure 2d–f**) or the sensitivity of $I_{Ca,L}$ to nifedipine (**Figure 4b,e**), among all developmental stages. These findings also appear to be consistent with the view that $Ca_V1.2$ channel primarily contributes to the functional $I_{Ca,L}$ in the mouse ventricle after birth.

The precise mechanisms underlying the postnatal developmental changes in the sensitivity of $I_{Ca,L}$ to inhibition by verapamil remain unclear. $I_{Ca,L}$ channel is composed of the α_1, $\alpha_2\delta$, and β subunits in the heart (1,2). Interestingly, patch-clamp experiments using heterologous expression systems have shown that α_{1C}/β_3 channel exhibits higher sensitivity to verapamil but a similar sensitivity to the dihydropyridine isradipine, compared with α_{1C} channel (40), suggesting that the subunit composition of $I_{Ca,L}$ channel substantially affects the sensitivity to inhibition by L-type Ca^{2+} channel antagonists (40,41). However, because the β_3 subunit is only expressed in the heart at the early embryonic stages, and not after birth (42), this possibility may not account for the postnatal developmental changes in the sensitivity of $I_{Ca,L}$ to verapamil. Future studies are thus required to elucidate the molecular basis for the postnatal developmental changes in the sensitivity of $I_{Ca,L}$ to inhibition by verapamil.

Three classes of L-type Ca^{2+} channel antagonists are known to exhibit different degrees of frequency-dependent block of $I_{Ca,L}$. Phenylalkylamines, such as verapamil and D600 (methoxy-verapamil), exhibit a marked frequency-dependent block of $I_{Ca,L}$ (31–33), which is assumed to arise from the preferential block of the channel in the open-state (43,44). In contrast, nifedipine shows tonic block of $I_{Ca,L}$ without an appreciable frequency-dependent block of $I_{Ca,L}$ (32). Diltiazem shows both tonic and frequency-dependent block of $I_{Ca,L}$ (31,32). In the present study, verapamil and diltiazem (**Figure 5c,e, and f**) but not nifedipine (**Figure 5d,f**) showed a frequency-dependent blocking action on $I_{Ca,L}$ in ventricular myocytes of both day 7 and 10–15-week mice. Given that the heart rate in neonates and infants is considerably higher than that in adults in humans, it is expected that inhibitory action of verapamil and diltiazem on $I_{Ca,L}$ becomes more potent in neonates and infants than in adults. Although diltiazem can

be safely used in infants in the clinical setting (10), verapamil produces a serious depression in the cardiac function of neonates and infants (4,6,7). Thus, it seems likely that the frequency-dependent blocking action on $I_{Ca,L}$ could not be a critical factor contraindicating its use in neonates and infants. It is thus expected that the higher sensitivity of $I_{Ca,L}$ to verapamil in neonates and infants (in comparison to adults) contributes to the serious depressant effects on the ventricular contractile function.

Limitations of the Study

We may assume that day 0 mice correspond to neonates in humans; days 7, 14, and 21 mice correspond to infants; day 28 mice correspond to children, and 10–15-week mice correspond to adults, based on the weaning age of postnatal day 21 in mice (23). However, the precise correlation in age-dependent development of the heart between mice and human has yet to be fully elucidated.

CONCLUSION

Our electrophysiological studies using a mouse heart model, have detected, for the first time, a higher sensitivity of ventricular $I_{Ca,L}$ to verapamil in neonatal and infant stages than in child and adult stages. This developmental change in the sensitivity of $I_{Ca,L}$ to verapamil is at least partly responsible for the verapamil-induced negative inotropic action observed in neonates and infants in the clinical setting.

SUPPLEMENTARY MATERIAL

Supplementary material is linked to the online version of the paper at http://www.nature.com/pr

STATEMENT OF FINANCIAL SUPPORT:

This study was supported by JSPS (The Japan Society for the Promotion of Science) KAKENHI Grant Number 25460287 and 17K08536 to H.M.

Disclosure: The authors declare no conflict of interest.

REFERENCES

1. Catteral WA. Structure and regulation of voltage-gated Ca^{2+} channels. Annu Rev Cell Dev Biol 2000;16:521–55.
2. Zamponi GW, Striessnig J, Koschak A, Dolphin AC. The physiology, pathology, and pharmacology of voltage-gated calcium channels and their future therapeutic potential. Pharmacol Rev 2015;67:821–70.
3. Opie LH. Calcium channel antagonists. Part III: Use and comparative efficacy in hypertension and supraventricular arrhythmias. Minor indications. Cardiovasc Drugs Ther 1988;1:625–56.
4. Kugler JD, Danford DA. Management of infants, children, and adolescents with paroxysmal supraventricular tachycardia. J Pediatr 1996;129:324–38.
5. Lee KL, Lauer MR, Young C, et al. Spectrum of electrophysiologic and electropharmacologic characteristics of verapamil-sensitive ventricular tachycardia in patients without structural heart disease. Am J Cardiol 1996;77:967–73.
6. Lapage MJ, Bradley DJ, Dick M 2nd. Verapamil in infants: an exaggerated fear? Pediatr Cardiol 2013;34:1532–4.
7. Epstein ML, Kiel EA, Victorica BE. Cardiac decompensation following verapamil therapy in infants with supraventricular tachycardia. Pediatrics 1985;75:737–40.
8. Sinaiko AR. Treatment of hypertension in children. Pediatr Nephrol 1994;8:603–9.
9. Flynn JT, Warnick SJ. Isradipine treatment of hypertension in children: a single-center experience. Pediatr Nephrol 2002;17:748–53.
10. Pass RH, Liberman L, Al-Fayaddh M, Flynn P, Hordof AJ. Continuous intravenous diltiazem infusion for short-term ventricular rate control in children. Am J Cardiol 2000;86:559–62.
11. Nakanishi T, Jarmakani JM. Developmental changes in myocardial mechanical function and subcellular organelles. Am J Physiol 1984;246: H615–25.
12. Tohse N, Seki S, Kobayashi T, Tsutsuura M, Nagashima M, Yamada Y. Development of excitation-contraction coupling in cardiomyocytes. Jpn J Physiol 2004;54:1–6.
13. Osaka T, Joyner RW. Developmental changes in calcium currents of rabbit ventricular cells. Circ Res 1991;68:788–96.
14. Huynh TV, Chen F, Wetzel GT, Friedman WF, Klitzner TS. Developmental changes in membrane Ca^{2+} and K^{+} currents in fetal, neonatal, and adult rabbit ventricular myocytes. Circ Res 1992;70: 508–15.
15. Hoshino S, Omatsu-Kanbe M, Nakagawa M, Matsuura H. Postnatal developmental decline in I_{K1} in mouse ventricular myocytes isolated by the Langendorff perfusion method: comparison with the chunk method. Pfügers Arch 2012;463:649–68.
16. Boerth SR, Zimmer DB, Artman M. Steady-state mRNA levels of the sarcolemmal Na^{+}-Ca^{2+} exchanger peak near birth in developing rabbit and rat hearts. Circ Res 1994;74:354–9.
17. Koban MU, Moorman AF, Holtz J, Yacoub MH, Boheler KR. Expressional analysis of the cardiac Na-Ca exchanger in rat development and senescence. Cardiovasc Res 1998;37:405–23.
18. Hamaguchi S, Kawakami Y, Honda Y, et al. Developmental changes in excitation-contraction mechanisms of the mouse ventricular myocardium as revealed by functional and confocal imaging analyses. J Pharmacol Sci 2013;123:167–75.
19. Chin TK, Friedman WF, Klitzner TS. Developmental changes in cardiac myocyte calcium regulation. Circ Res 1990;67:574–9.
20. Chin TK, Christiansen GA, Caldwell JG, Thorburn J. Contribution of the sodium-calcium exchanger to contractions in immature rabbit ventricular myocytes. Pediatr Res 1997;41:480–5.
21. Boucek RJ Jr, Shelton M, Artman M, Mushlin PS, Starnes VA, Olson RD. Comparative effects of verapamil, nifedipine, and diltiazem on contractile function in the isolated immature and adult rabbit heart. Pediatr Res 1984;18:948–52.
22. Seguchi M, Jarmakani JM, George BL, Harding JA. Effect of Ca^{2+} antagonists on mechanical function in the neonatal heart. Pediatr Res 1986;20:838–42.
23. König B, Markl H. Maternal care in house mice. Behav Ecol Sociobiol 1987;20:1–9.
24. Sengupta P. The laboratory rat: relating its age with human's. Int J Prev Med 2013;4:624–30.
25. Shioya T. A simple technique for isolating healthy heart cells from mouse models. J Physiol Sci 2007;57:327–35.
26. Kojima A, Kitagawa H, Omatsu-Kanbe M, Matsuura H, Nosaka S. Ca^{2+} paradox injury mediated through TRPC channels in mouse ventricular myocytes. Br J Pharmacol 2010;161:1734–50.
27. Hamill OP, Marty A, Neher E, Sakmann B, Sigworth FJ. Improved patch-clamp techniques for high-resolution current recording from cells and cell-free membrane patches. Pflügers Arch 1981;391: 85–100.
28. Kojima A, Kitagawa H, Omatsu-Kanbe M, Matsuura H, Nosaka S. Inhibitory effects of sevoflurane on pacemaking activity of sinoatrial node cells in guinea-pig heart. Br J Pharmacol 2012;166:2117–35.
29. Bénitah JP, Gomez AM, Bailly P, et al. Heterogeneity of the early outward current in ventricular cells isolated from normal and hypertrophied rat hearts. J Physiol 1993;469:111–38.
30. Grandy SA, Trépanier-Boulay V, Flset C. Postnatal development has a marked effect on ventricular repolarization in mice. Am J Physiol Heart Circ Physiol 2007;293:H2168–77.

31. Lee KS, Tsien RW. Mechanism of calcium channel blockade by verapamil, D600, diltiazem and nitrendipine in single dialysed heart cells. Nature 1983;302:790–4.
32. Uehara A, Hume JR. Interactions of organic calcium channel antagonists with calcium channels in single frog atrial cells. J Gen Physiol 1985;85:621–47.
33. Nawrath H, Wegener JW. Kinetics and state-dependent effects of verapamil on cardiac L-type calcium channels. Naunyn Schmiedebergs Arch Pharmacol 1997;355:79–86.
34. Takemura H, Yasui K, Opthof T, et al. Subtype switching of L-type Ca^{2+} channel from $Ca_v1.3$ to $Ca_v1.2$ in embryonic murine ventricle. Circ J 2005;69:1405–11.
35. Qu Y, Karnabi E, Ramadan O, Yue Y, Chahine M, Boutjdir M. Perinatal and postnatal expression of $Ca_v1.3$ α_{1D} Ca^{2+} channel in the rat heart. Pediatr Res 2011;69:479–84.
36. Redfern WS, Carlsson L, Davis AS, et al. Relationships between preclinical cardiac electrophysiology, clinical QT interval prolongation and torsade de pointes for a broad range of drugs: evidence for a provisional safety margin in drug development. Cardiovasc Res 2003;58:32–45.
37. Qu Y, Boutjdir M. Gene expression of SERCA2a and L- and T-type Ca channels during human heart development. Pediatr Res 2001;50:569–74.
38. Lipscombe D, Helton TD, Xu W. L-type calcium channels: the low down. J Neurophysiol 2004;92:2633–41.
39. Sinnegger-Brauns MJ, Huber IG, Koschak A, et al. Expression and 1,4-dihydropyridine-binding properties of brain L-type calcium channel isoforms. Mol Pharmacol 2009;75:407–14.
40. Lacinová L, Ludwig A, Bosse E, Flockerzi V, Hofmann F. The block of the expressed L-type calcium channel is modulated by the β_3 subunit. FEBS Lett 1995;373:103–7.
41. Mitterdorfer J, Froschmayr M, Grabner M, Striessnig J, Glossmann H. Calcium channels: the β-subunit increases the affinity of dihydropyridine and Ca^{2+} binding sites of the α_1-subunit. FEBS Lett 1994;352:141–5.
42. Link S, Meissner M, Held B, et al. Diversity and developmental expression of L-type calcium channel β2 proteins and their influence on calcium current in murine heart. J Biol Chem 2009;284:30129–37.
43. Hockerman GH, Johnson BD, Scheuer T, Catterall WA. Molecular determinants of high affinity phenylalkylamine block of L-type calcium channels. J Biol Chem 1995;270:22119–22.
44. Tang L, Gamal El-Din TM, Swanson TM, et al. Structural basis for inhibition of a voltage-gated Ca^{2+} channel by Ca^{2+} antagonist drugs. Nature 2016;537:117–21.